II INTERNATIONAL SCIENTIFIC CONVENTION
"II ICC UCLV 2019"

JUNE 23th – 30th, 2019
CAYOS DE VILLA CLARA. CUBA.

COMEC 2019

Peak pressures at the throttled flow of oscillating valves

Dario Alviso[1], Denisse Sciamarella[2], Yann Fraigneau[3], Guillermo Artana[1]

1- LFD, Facultad de Ingeniería, Universidad de Buenos Aires, CONICET, Argentina

2- Institut Franco-Argentin d'Études sur le Climat et ses Impacts (IFAECI), UMI 3351 (CNRS-CONICET-UBA),C1428EGA CABA, Argentina

3- LIMSI-CNRS, BP 133 - F 91403 ORSAY Cedex, FRANCE

Abstract: *Pressure signals measured at the throttled flow of oscillating valves show a double peak when the closing and reopening of the clearance occur in short times. This phenomenon has been evidenced in spring-loaded valves or in valves of biological flows such as vocal-fold collision upon glottal flow. A comprehensive study of the fluid dynamical causes of this flow behavior is still pending. This work considers a valve with a simple geometry and a prescribed evolution of gap height with time. High performance numerical simulations in two dimensions and simplified models are used to explain experimental results and undertake a parametric study. A reversal of the longitudinal volumetric flow direction near the entrance and exit of the channel at closing and reopening, named suction-cup effect, is shown to be associated to the double peak presence in pressure signals.*

Keywords: *Valves, Vocal-folds, Stream filament theory, 2D Direct numerical simulations, Lubrification theory*

1. Introduction

Valves are critical components in industrial processes. Whereas they are often designed to be replaceable and inexpensive, valve failures can cause costly shutdowns in addition to safety hazards in certain applications [1]. Due to the complex fluid-structure interaction, valve systems have a tendency to self-oscillate and such dangerous oscillations are challenging to predict in the design phase [2]. Oscillations of different valve systems have been studied by several authors, e.g. in spring-loaded valves [1, 2, 3,

4], plug valves [5, 6], compressor valves [7], ball valves [8], pilot-operated two-stage valves [9, 10], relief valves [11, 12] and control valves [13, 14, 15, 16, 17, 18].

Particularly, spring-loaded valves functioning are prone to be altered by vibrations. The support of the moving part of the valve is inherently flexible and flow occurs through small openings, and hence their operation is more likely to be influenced by the interaction of the body with the fluid flow [1]. Flow-induced vibration (FIV) is an important concern for the operation of these valves, not only because it produces oscillations of the flow area but also because it shortens the life of the valve. [1]. Thus, it is not surprising that several studies of FIV on valves were carried out for spring-loaded systems. For instance, an experimental characterization of the self-excited vibrations of spring-loaded valves was realized by Bouzidi et al. [1], considering the self-excitation mechanism on a model spring-loaded valve with an emphasis on the interaction between the system flow and sound fields, and the valve structure. Moreover, a model reduction of a direct spring-loaded pressure relief valve with upstream pipe was studied by Hos et al. [2]. In addition, dynamic behavior of direct spring loaded pressure relief valves in gas service was performed by Hos et al. [3]. Laboratory experiments results with varying mass flow rates and length of inlet pipe were presented for three different commercially available valves.

Detailed experimental studies describing the evolution with time of flow parameters when the gap height is reaching zero are quite scarce. One of the few works studying this phenomenon was presented by D'Netto and Weaver [5]. Therein, divergence and limit cycle oscillations in valves operating at small openings were studied both experimentally and theoretically. In the experiments, instantaneous pressure drop, flow velocity immediately downstream of the valve, and valve displacement were recorded during limit cycle oscillations. The effects of valve initial opening displacement, valve restraint stiffness and fluid inertia were investigated. Remarkably, a double-peak in pressure signals at the gap for different operating conditions (initial opening, stiffness and downstream pipe-length) was systematically found when the height is reaching zero.

In the voice production system, the human vocal folds act as a self-oscillating valve which induces pressure waves upstream and downstream from the glottis in a water-hammer mechanism [19]. At the intraglottal space (gap of the valve) a double-peak in the time-pressure signals may take place as the separation of vocal folds are close to a zero value (vocal fold collision). Also, as for mechanical valves, experimental studies related to intraglottal flow behavior upon vocal-fold collision are scarce, nonetheless some measurements of intraglottal pressure in replicas of the vocal folds were reported by Deverge et al. [20]. The authors in this work report the pressure evolution for the straight uniform replicas driven by a mechanical system. They show signals with the double-peak at the collision phase and illustrate that this phenomenon was not captured by using simple models. The best results found by these authors were attained using a model based in a lubrification theory approximation. This approach combines the assumption of a quasiparallel flow together with the assumption that inertial effects are negligible. The authors also indicate that a model based on an inviscid unsteady approximation fails to explain the measured data.

In order to analyze the physics associated to the double peak, we will show a study based on a numerical study with simulations using high performance computational fluid dynamics in two spatial dimensions and the experimental conditions reported in Deverge et al. [20]. As we will show, the adopted numerical approach shows satisfactory results in agreement with experiments. There is also an interest to dispose simplified models of fluid behaviour to analyze the oscillations of valves. To this end, we consider in this work a one-dimensional model of the flow unsteadiness based on the stream filament theory [21]. This last simple model considers the flow as inviscid and emphasizes the effect of unsteady terms in conservation equation. We will show that this model provides satisfactory results unlike in Deverge et al. [20]. A comparison with the model inspired on lubrification theory described in Deverge et al. [20] will also be presented.

2. Geometric configuration of the study

The experimental valve configuration setup from Deverge et al. [20] was chosen in the present paper as is one of the simplest geometrical configuration that enables to analyze

the behavior in the gap. Even though this is a quite simple geometric configuration, the physical problem related to the closure and opening of the gap is expected to be similar to that observed in the cases of valves of more complex geometry considered in other studies in which the double-peak in pressure has been observed [5].

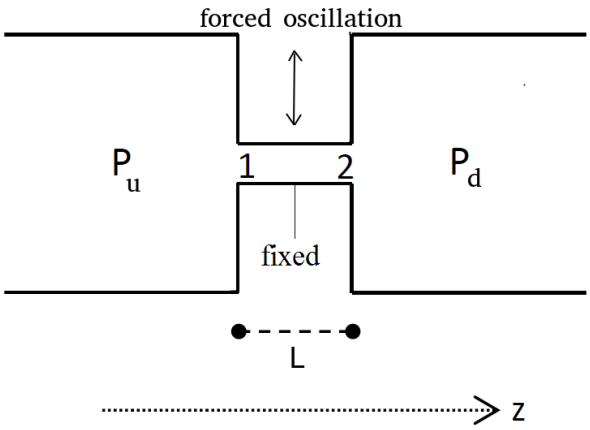

Fig. 1 Scheme of the frontal section, with P u and P d the upstream and downstream pressures, and L the mass length. The lower mass is maintained fixed while the upper has a prescribed vertical movement.

A geometrical sketch of the configuration of the study is given in Fig. 1, where Pu denotes upstream pressure (equal to 1500 Pa unless stated otherwise), Pd denotes the downstream pressure (equal to 0 Pa unless stated otherwise), L (2 cm) is the channel length in the stream-wise direction z and the width in the perpendicular direction is Lg = 3 cm. The gap height is variable following an approximate sinus law with time. A typical value of the amplitude of this oscillation is 1mm. Note that the scheme of Fig. 1 is not to scale. As shown in the figure, the lower mass cannot move while the upper one oscillates vertically with a prescribed frequency. The frequency imposed to the upper mass movement determines the suddenness of the valve closure and a typical value for these experiment was 35 Hz. Typical values of Re for the experiment considered are close to 45000.

In order to model the flow behavior near the gap closure and immediate reopening, two approaches were chosen : a 2D DNS numerical simulation and 1D numerical models

based on the stream filament theory (SFM) and lubrification theory (LT). These points will be detailed in the next sections.

3. 2D Direct numerical simulations

The problem is addressed in two spatial dimensions for the sake of simplicity, assuming that three-dimensional effects should not be dominant upon closure. The numerical method implemented to solve the Navier-Stokes equations is based on the usual projection method, according to the delta form approach. For more information, the reader is directed to the works of [22-25].

4. Simplified fluid dynamics models

4.1. Lubrification theory approach

We succinctly explain the basis of the lubrification model proposed by Deverge et al. As we signaled above, this approach combines the assumption of a quasi-parallel flow together with the assumption that inertial effects are negligible. As the pressure forces balance the viscous ones, the velocity profile in the different positions of the channel may be approximated with the Poiseuille expression [20, 29] :

$$u(x,y) = -\frac{1}{2\rho\nu}\frac{\partial p(x)}{\partial x}(h-y)y$$

The integration of this profile at a given position gives the local flow rate that depends on the local pressure gradient. Then, considering the mass conservation equation it is possible to obtain after integration :

$$p(x) - p_u = \left(\frac{p_d - p_u}{L}\right)x + \frac{12\rho\nu}{h^3}\left(\frac{dh}{dt}\right)\frac{x(x-L)}{2}$$

With this last expression, and for a prescribed time dependence of the height, it is possible to determine for each stream-wise position the pressure value.

4.2. 1D Stream filament model

Most of the vocal-fold models consider glottal flow in terms of a steady air velocity that is single-valued along the glottis [30], so that flow fluctuations are directly and entirely determined by the fluctuations of the channel area. The throttled flow model that we propose here is in line with other works [31, 32], which considered the flow in this

biological oscillating valves and asserted that unsteadiness cannot be neglected throughout the cycle to describe the dynamics of the oscillations.

We will assume neither quasi-steadiness nor stream-wise uniformity of the flow magnitudes. The complexity remains however moderate : unsteady acceleration is limited to the contribution of the unidirectional wall motion and the problem of flow separation position [33] is ruled out. We shall apply the stream filament theory under the assumption of incompressibility of the flow [21]. Flow quantities are functions both of time and of the length along the streamline, so that :

$$F(t) = L_g \int_0^L P(z,t)\,\mathrm{d}z,$$

$$P(z,t) = P_0 - \rho\left(\frac{1}{2}U^2(z,t) + \int_0^z \partial_t U(z,t)\,\mathrm{d}z\right).$$

Here, Lg is the size of the channel in the direction that is normal to the plane of Fig. 1, P(z,t) is the intravalve pressure, U(z,t) the air velocity, ρ the air density, z the streamwise coordinate and t time.

Actually, the section of the stream-tube inside the channel is not strictly constant because of the growth of the boundary layer of the flow inside the channel [20, 34]. Including the dynamics of an unsteady boundary layer between the oscillating walls of a channel is however not a simple task : this supplementary source of complexity is thus expressly left out of this derivation.

The continuity equation in the context of stream filament theory is presented for the section of the stream-tube [21] :

$$\int_z^L \partial_t \rho a(z,t)\,\mathrm{d}z + \rho_2 U_2 a_2 - \rho_1 U_1 a_1 + \iint_{S_\omega} \rho \vec{u}\cdot\vec{n}\,dS = 0,$$

where a(z, t) denotes the cross-sectional area and u.n is the normal component of the flow velocity at the moving wall.

As the cross-section of the tube does not change in time the integral over the wall Sω vanishes, and the continuity equation between an arbitrary point within the channel (labeled 1) and at the exit (labeled 2) is written as follows (Fig. 1) :

$$\int_z^L \partial_t a(z,t)\,\mathrm{d}z + U_2 a_2 - U_1 a_1 = 0,$$

$$U(z,t) = U_2(t) + \frac{\int_z^L \partial_t a(z,t)dz}{a(z,t)}$$

An additional requirement results from the boundary condition is P(z2,t) = Pi. This boundary condition disregards the problem of unsteadiness at the discharge. As mentioned in the introduction, the model retains a single source of unsteadiness related to wall motion. Furthermore, as the upper mass oscillation is driven by a motor, a(z, t) is obtained from the experimental measurements of the channel height found in [20]. It must be pointed out that the flow rate Q(t) ≡ Q2(t) = a(t)*U2(t) at the exit is time-varying due to the combined fluctuations in gap area and air velocity at the exit.

4. Results

4.1. Analysis at closing and reopening

The upper frame of Fig. 2 shows a typical evolution with time of the valve clearance considered in this work. It has been measured for a given operation of the device (35 Hz and non dimensional oscillation amplitude dh/L of 0.05) by Deverge et al. [20]. The lower frame of Fig. 2 shows the pressure evolution with time recorded for the same experimental condition. This last figure shows a grey shaded region in correspondence with the interval of time when masses are in contact. We observe that excluding this zone, and taking into account instants immediately before and immediately after it, pressure respectively rises and diminishes abruptly, being observed then the phenomenon of double peak in pressure signal. It is then of interest here to propose a comparison between the experimental results (Deverge et al. [20]) and those issued by the models considered in this work (2D DNS, LT and SFM).

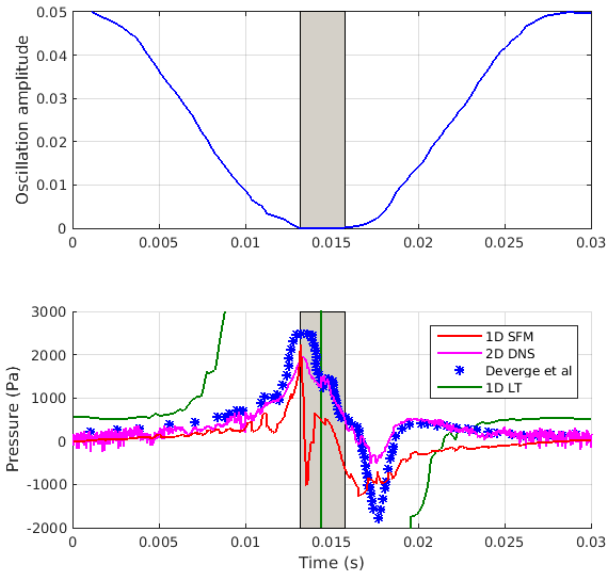

Fig. 2 Comparison of the experimental (Deverge et al. [20]) and numerical (1D SFM, 2D DNS and 1D LT) pressure signals, for one cycle.

The performance of all the models for the grey shaded zone, when the two masses are in contact, is difficult to analyze, as the experimental and numerical values during the collision are questionable results from a physical point of view. Experimentally, in this interval of time, negligible air flux is passing through the channel and the signal recorded by the sensor is quite difficult to link to a fluid dynamic behaviour. Concerning the modelling, 2D DNS simulations were carried out with a variable number of points in the mesh. When masses are in contact, this modelling is performed without a full closure but with an almost negligible gap. Hence, the number of mesh points are reduced drastically and local numerical fluctuations were observed in this interval. These fluctuations however do not seem to affect the description of the double peak in pressure. Concerning SFM simulations, as the clearance becomes quite small, so does the denominator of the SFM Equation. To avoid possible divergence of the model during numerical calculations, an artificial minimum value of gap height is forced (the gap height is of the magnitude order of the masses material roughness). This correction does not seem enough to solve the divergence problem of the LT approach in this region.

Outside this shaded region but in the proximity of it, the figure reveals that DNS and SFM predictions are consistent with the experimental results. The shapes of the curves and values adopted by pressure are in a relatively good agreement with the experiments. DNS and SFM can be considered as good approximations that capture the essential aspects of closure/reopening flow dynamics, while the results of the LT model, even though they are consistent with those of Deverge et al. [20], are much less satisfactory. We observe that LT captures the change in the pressure signal, but it largely overestimates the magnitude of the peaks. Thus, in what follows, only the two models that could be satisfactorily validated will be considered.

5.2. "Suction-cup" effect

Figure 3 presents contour maps for the pressure signals (left) and volumetric flow Q (right) with 2D DNS along the channel length. In the left figure, just before the valve closure (and right after), there is a change in the pressure field. As the gap height diminishes, vortices tend to disappear and the flow has laminar characteristics with instantaneous velocity distributions similar to those of a steady flow that takes place in a narrow channel with a decreasing pressure gradient. However, this configuration changes immediately before closure and after reopening. Prior to the total closure, a localized overpressure is first observed in the upstream region of the channel, followed at the reopening by a localized depression in the downstream region. The pressure gradient is no longer constant and changes its sign at the interior of the channel. The right figure 3 illustrates that this process is accompanied by a reversal of the flow at the channel ends. This flow reversal is hereafter labeled "suction-cup" effect. During closure, an exhaust of the air occupying the gap is produced and a fraction of this air volume that cannot attain the downstream exit section is pushed out through the inlet by the oscillating mass. During the reopening, the refilling of the gap with air cannot be entirely produced through the inlet, and air is aspirated through the exit section of the channel. The suction-cup effect thus depends on the valve dynamics that is imposed, as well as on the flow conditions. In the case examined, due to the low value of oscillation amplitude, the reversal remains very limited in time and the volumetric flows are very low. We will extend the analysis to other dynamical conditions of oscillations in next

paragraphs to illustrate in more detail this behavior. Fig. 2 illustrates that the SFM reproduces the values of pressure at the mid-channel quite well. It may be of interest here to analyze if SFM reproduces the results of distributions of the pressure and the

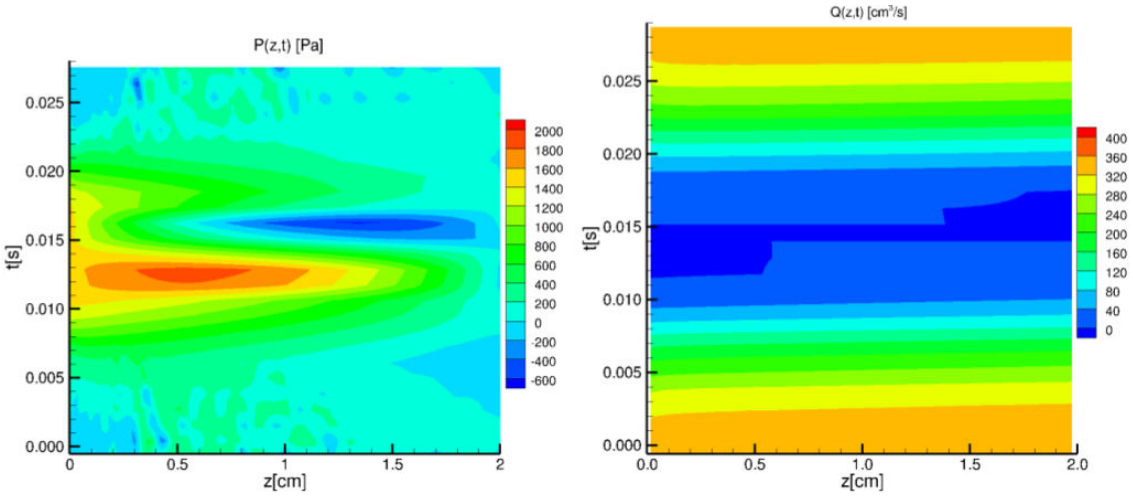

flow rate along the channel obtained with the high performance numerical simulations.

Fig. 3 Contour maps for the pressure P (max= 1876, min= -615 Pa) and volumetric flow Q (max= 353.7, min= -2.33 cm 3 /s) in the 2D DNS along the channel length, at 35 Hz and dimensionless oscillation amplitude of 0.05 (dh/L).

Fig. 4 shows results issued from the SFM presented as contour maps for the pressure P and volumetric flow Q along the channel length, for one cycle of oscillation to be compared with the results of Fig. 3. Concerning the pressure results, it is shown that the pressure distributions with SFM and DNS are not coincident. Even though similar trends are observed during closure, the minimum of pressure during the reopening phase is displaced upstream. This effect however does not bring strong consequences on the flowrate distribution. As a consequence of wall shear absence, SFM predicts larger values of flow rates but the spatial and temporal distribution of flowrates trends are rather coincident with both approaches. The right Fig. 4 shows the reversal of the flow at the channel ends (Q becomes negative at both the upstream and downstream parts of the channel). Hence, the model captures the "suction-cup" effect and seems to be not significantly dependent on the inclusion of viscous effects.

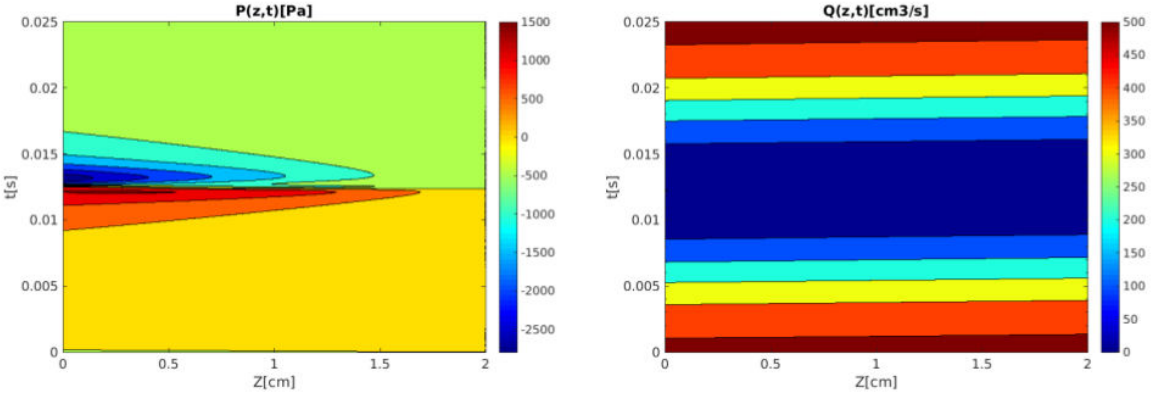

Fig. 4 Contour maps for the pressure P (max= 1536, min= -2796 Pa) and volumetric flow Q (max= 515.64, min= -0.01 cm 3 /s) with the SFM along the channel length, at 35 Hz and dimensionless oscillation amplitude of 0.05 (dh/L).

5.3. Non-dimensional number of interest

We propose a study in order to find out what the key parameters are in the "suction-cup" effect and the associated double-peak pressure signal. To this end we will consider results issued from SFM to avoid the large time consuming required with the DNS. It is natural to consider first here Strouhal number defined as :

$$St = \frac{v/\tau}{v.v/L}$$

And the ratio of Euler and Strouhal numbers as :

$$\frac{Eu}{St} = \frac{P_u - P_d}{\rho L f^2 H}$$

The ratio of Euler and Strouhal numbers correlates the pressure and local inertial forces, and evidences parameters that are dominant in the reversal of the flow phenomena : the upstream and downstream pressure (Pu and Pd, respectively), the density (ρ), the channel length (L), the frequency (f) and amplitude (H) of the oscillations. We have considered different ratios of Eu/St by setting different dynamics of oscillation (determined by H and f) and analyzing with SFM the volumetric flow fields. Table 1 presents the results for different frequencies of oscillation when values of upstream-downstream pressure difference Pu − Pd = 500, 1000 and 1500 Pa, and amplitude (H), density (ρ) and the channel length (L) were kept constant. This table shows that for Pu − Pd = 500 Pa, flow reversal begins for Eu/St ratio of about ~ 52000-53700 (for higher

Eu/St, all the values in the volumetric flow field are positive and consequently there is no flow reversal). As the Eu/St ratio decreases (local inertial forces become more important), the flow reversal increases (higher negative volumetric flow), up to a Eu/St ratio of about ~ 7500, when negative velocities are of the same magnitude order as the positive velocities, which is the limit of convergence of the simulations. In order to verify that for others pressure conditions (Pu-Pd), the same Eu/St ratio is found, the parametric studies of frequency were extended using SFM, for Pu-Pd = 1000 and 1500 Pa. As it can be seen in the table, flow reversal begins for Eu/St ratio of about ~ 50700-53700 in all cases. For these values of pressure difference also as Eu/St ratio decreases,

Frequency variation (H constant)

$P_u - P_d$= 500 Pa			$P_u - P_d$= 1000 Pa			$P_u - P_d$= 1500 Pa			
H (mm)	f (Hz)	Eu/St	H (mm)	f (Hz)	Eu/St	H (mm)	f (Hz)	Eu/St	Observation
1	>20.5	52182	1	>29	52151	1	>35	53700	Begins flow reversal
1	<54	7520	1	<77	7397	1	<95	7289	Very high flow reversal
1.5	>16.5	53700	1.5	>24	50763	1.5	>29	52151	Begins flow reversal
1.5	<44	7551	1.5	<63	7367	1.5	<77	7397	Very high flow reversal

TABLE 1: Parametric study of frequency using SFM, for upstream pressure $P_u - P_d$= 500, 1000 and 1500 Pa.

the flow reversal increases, up to a Eu/St ratio of about ~ 7280-7450.

Tab. 2 presents results when varying the value of oscillation amplitude (H), for cases with a pressure difference Pu-Pd = 500, 1000 and 1500 Pa. Compared to the previous results, we obtained that the Eu/S t ratios for which flow reversal limits are similar (upper ~ 52600, lower 7200-7450). Hence, within our experimental conditions, the range of Eu/S t ratios in which it may be observed the flow reversal (and double peak in the pressure signal) is ~ 7200-53700.

H variation (frequency constant)

$P_u - P_d$= 500 Pa			$P_u - P_d$= 1000 Pa			$P_u - P_d$= 1500 Pa			
H (mm)	f (Hz)	Eu/St	H (mm)	f (Hz)	Eu/St	H (mm)	f (Hz)	Eu/St	Observation
>0.34	35	52652	>0.7	35	51148	>1	35	53700	Begins flow reversal
<2.4	35	7459	<4.8	35	7459	<7.3	35	7356	Very high flow reversal
>0.085	70	52600	>0.17	70	52652	>0.25	70	53700	Begins flow reversal
<0.615	70	7277	<1.2	70	7459	<1.8	70	7459	Very high flow reversal

TABLE 2: Parametric study of oscillation amplitude (H) using SFM, for upstream pressure $P_u - P_d$= 500, 1000 and 1500 Pa.

6. Conclusions

This work proposes an analysis of geometrically simple oscillating valves, exhibiting a double peak in the pressure signal.

We have modeled the flow physics with a high performance numerical code in two dimensions (2D DNS) and with the restriction of one-dimensional flow imposed by the stream filament theory (SFM). Results were also compared with those of the lubrification theory (LT) previously proposed by other authors. A validation of the different approaches was performed by comparing the pressure signals at the mid-channel position of experiments and those obtained with the different models. With 2D DNS and SFM simulations a relatively good agreement was observed, whereas LT results were much less satisfactory. It was found that, at instants immediately preceding the closure of the valve, the fluid may be expelled from the upstream and downstream ends of the channel. This occurs even when global pressure gradients (calculated with upstream and downstream atmospheres) oppose to this flow. This effect is similar as the one produced by some "suction-cup" devices.

Also, just before the closure (and right after reopening starts), important changes may appear in the pressure field in the channel. During closure, the flow inside the channel changes from an almost constant gradient configuration (in agreement with a Poisseuile type flow), to a situation where there is a localized overpressure in the upstream part of the channel. At the reopening phase, the fluid refills the gap and a localized depression in the downstream part of the channel takes place. These localized inverse pressure gradients can be accompanied by a reversal of the flow at the channel ends. The overpressure before the closure is accompanied by a negative volumetric flow at the upstream part of the channel; and the depression after the closure by a negative volumetric flow at the downstream part of the channel. We observed that when the double-peak in the pressure signal takes place, it is accompanied by these flow reversals.

The comparison of results of DNS and SFM of spatio-temporal pressure distributions show some differences especially in the downstream region. On the contrary, even though the SFM overestimates the maximum values of flow rates, the spatio-temporal volumetric flow fields are in relative good agreement, and results of flow reversal are similar.

The ratio of Euler and Strouhal numbers correlate the key forces (pressure and local inertial forces) and flow reversal occured within a range of values of this ratio. Flow reversal appears when the Eu/St ratio ~50700-53700, and increases as this ratio decreases up to a value of about ~7280-7450, which is the limit of convergence of the simulations.

7. Bibliographical references

[1] S. E. Bouzidi, M. Hassan, S. Ziada, Journal of Fluids and Structures 76 (2018) 558 - 572.

[2] C. Hos, C. Bazso, A. Champneys, IMA Journal of Applied Mathematics 80 (2015) 1009–1024.

[3] C. Hos, A. Champneys, K. Paul, M. McNeely, Journal of Loss Prevention in the Process Industries 31 (2014) 70 – 81.

[4] S. E. Bouzidi, M. Hassan, S. Ziada, Journal of Fluids and Structures 83 (2018) 72 – 90.

[5] W. D'Netto, D. Weaver, Journal of Fluids and Structures 1 (1987) 3–18.

[6] F. Inoue, E. Outa, H. Matsuoka, T. Machiyama, Flow oscillation in a contoured-plug valve with multi-hole retainer and the related string cavitation generation, 1991.

[7] R. Habing, M. Peters, Journal of Fluids and Structures 22 (2006) 683 – 697.

[8] A. Nayfeh, H. Bouguerra, International Journal of Non-Linear Mechanics 25 (1990) 433 – 449.

[9] K. Botros, G. Dunn, J. Hrycyk, ASME. Journal of Fluids Engineering 119 (1997) 671–679.

[10] Q. Ye, J. Chen, Simulation Modelling Practice and Theory 17 (2009) 794 – 816.

[11] G. Makaryants, ICSV 2016 - 23rd International Congress on Sound and Vibration : From Ancient to Modern Acoustics (2016).

[12] D. Galbally, G. García, J. Hernando, J. Sánchez, M. Barral, Nuclear Engineering and Design 293 (2015) 258–271.

[13] A. Misra, K. Behdinan, W. Cleghorn, Journal of Fluids and Structures 16 (2002) 649 – 665.

[14] K. Yonezawa, R. Ogawa, K. Ogi, T. Takino, Y. Tsujimoto, T. Endo, K. Tezuka, R. Morita, F. Inada, Journal of Fluids and Structures 35 (2012) 76 – 88.

[15] M. V. Balyaba, M. A. Ermilov, A. N. Kryuchkov, Procedia Engineering 176 (2017) 577 – 585. Proceedings of the 3rd International Conference on Dynamics and Vibroacoustics of Machines (DVM2016) June 29–July 01, 2016 Samara, Russia.

[16] T. Wang, L. Xie, F. Tan, H. Su, IFAC-PapersOnLine 48 (2015) 433 – 438. 9th IFAC Symposium on Advanced Control of Chemical Processes ADCHEM 2015.

[17] L. Fang, J. Wang, X. Tan, IEEE/ASME Transactions on Mechatronics 21 (2016) 2773–2783.

[18] R. Morita, F. Inada, M. Mori, K. Tezuka, Y. Tsujimoto, Nihon Kikai Gakkai Ronbunshu, B Hen/Transactions of the Japan Society of Mechanical Engineers, Part B 72 (2006) 634–641.

[19] N. H. Fletcher, The Journal of the Acoustical Society of America 93 (1993) 2172–2180.

[20] M. Deverge, X. Pelorson, C. Vilain, P. Y. Lagree, F. Chentouf, J. Willems, A. Hirschberg, J. Acoust. Soc. Am. 114 (6) (2003) 3354–3362.

[21] J. H. Spurk, Fluid Mechanics, Berlin Heidelberg, pp. 261–276.

[22] J. Guermond, P. Minev, J. Shen, Computer Methods in Applied Mechanics and Engineering 195 (2006) 6011 – 6045.

[23] K. Goda, Journal of Computational Physics 30 (1979) 76 – 95.

[24] D. W. Peaceman, H. H. R. JR., J. Soc. Indust. Appl. Math. 3 (1955).

[25] R. Pasquetti, R. Bwemba, L. Cousin, Applied Numerical Mathematics 58 (2008) 946 – 954. Spectral Methods in Computational Fluid Dynamics.

[26] C. S. Peskin, Acta Numerica 11 (2002) 479–517.

[27] R. Mittal, G. Iaccarino, Annual Review of Fluid Mechanics 37 (2005) 239–261.

[28] B. Kadoch, D. Kolomenskiy, P. Angot, K. Schneider, Journal of Computational Physics 231 (2012) 4365 – 4383.

[29] S. H., G. K., Boundary layer theory, 2000.

[30] I. R. Titze, J. Acoust. Soc. Am. 83 (4) (1988) 1536–1552.

[31] M. Krane, T. Wei, J. Acoust. Soc. Am. 120 (3) (2006) 1578–1588.

[32] M. Krane, M. Barry, T. Wei, J. Acoust. Soc. Am. 128 (1) (2010) 372–383.

[33] D. Sciamarella, P. Le Quéré, European Journal of Mechanics - B/Fluids 27(1) (2008) 42–53.

[34] K. Ishizaka, J. L. Flanagan, Speech Commun. Res. Lab. Monograph 8 (1972) Santa Barbara, CA.